American Journal of
Biomedical Science & Research

www.biomedgrid.com
ISSN: 2642-1747

Research Article

Mechanism Analysis of Modified Naoxintong in the Prevention and Treatment of Hyperlipidemic Atherosclerosis Based on Network Pharmacology

Jiren Zhang[1,2*], Junjie Hao[3], Yang Zhang[2],Yuan Wei[1], Yuxuan Liu[4] and Leiming Wang[2]

[1]*Guangzhou Yiwen Naoxinkang Medical Research Center, China*

[2]*Shanghai chenhe Life Sciences Research Center, Shanghai, China*

[3]*HJ healthcare and biological technology, Katy,77494. TX. USA*

[4]*Guangdong Food and Drug Vocational College School of Nursing, China*

***Corresponding author:** Jiren Zhan, Guangzhou Yiwen Naoxinkang Medical Research Center, Shanghai chenhe Life Sciences Research Center, Shanghai, China.

To Cite This article: *Jiren Zhang*, Junjie Hao, Yang Zhang,Yuan Wei, Yuxuan Liu and Leiming Wang, Mechanism Analysis of Modified Naoxintong in the Prevention and Treatment of Hyperlipidemic Atherosclerosis Based on Network Pharmacology. Am J Biomed Sci & Res. 2026 31(4) AJBSR.MS.ID.004067,* **DOI:** 10.34297/AJBSR.2026.31.004067

Received: June 26, 2026 **Published:** July 07, 2026

Abstract

Objective: The modified Naoxintong (NXT) is composed of Rhodiola rosea, *Crataegus pinnatifida, Pueraria lobata, Curcuma longa*, Sophora japonica flower bud, astaxanthin, coenzyme Q10, Astragalus membranaceus, red yeast rice and nattokinase. Preclinical studies have indicated its potential effects on lipid regulation, anti-inflammation, anti-oxidation and anti-atherosclerosis. This study adopted network pharmacology and molecular docking techniques to systematically explore the active ingredients, core targets and key signaling pathways of the modified formula against Hyperlipidemic Atherosclerosis (HLA), and to construct a multi-dimensional regulatory network of "ingredient-target-pathway".

Methods: Active ingredients were collected from TCMSP, PubChem and relevant literatures. Targets of ingredients were predicted using SwissTargetPrediction and TCMSP databases. HLA-related targets were retrieved from GeneCards, OMIM and DisGeNET databases by intersecting targets of hyperlipidemia and atherosclerosis. Intersection targets between drug and disease were obtained. The Protein-Protein Interaction (PPI) network was established via STRING, and core targets were screened through topological analysis in Cytoscape. Gene Ontology (GO) and Kyoto Encyclopedia of Genes and Genomes (KEGG) enrichment analyses were performed using DAVID with a False Discovery Rate (FDR) < 0.05 as the significant threshold. AutoDock Vina was applied for molecular docking between core ingredients and core targets, and a binding energy ≤ -5.0 kcal·mol^{-1} was defined as favorable binding activity.

Results: A total of 86 active ingredients were screened out, corresponding to 398 drug targets. After intersecting with 372 HLA-related disease targets, 131 potential therapeutic targets were acquired. Sixteen core targets including AKT1, TP53, TNF, IL6, STAT3, MAPK1, VEGFA, SREBF1 and HMGCR were identified via PPI network analysis. GO enrichment results revealed that these targets were mainly involved in lipid metabolism, cholesterol homeostasis, inflammatory response regulation, oxidative stress response and foam cell differentiation. KEGG enrichment yielded 42 significantly enriched pathways (FDR < 0.05), among which the core pathways included PI3K-Akt signaling pathway, mTORC1-SREBPs signaling network, AGE-RAGE signaling pathway, NF-κB signaling pathway, Nrf2-mediated anti-oxidative pathway, TNF signaling pathway and arachidonic acid metabolism pathway. Molecular docking results showed that monacolin K from red yeast rice bound to HMGCR with a binding energy of -9.8 kcal·mol^{-1}, curcumin bound to AKT1 with a binding energy of -10.2 kcal·mol^{-1}, and astaxanthin bound to Nrf2 with a binding energy of -8.3 kcal·mol^{-1}, verifying the high affinity between active ingredients and core targets.

Conclusion: The modified Naoxintong exerts therapeutic effects on hyperlipidemic atherosclerosis through a four-way synergistic mechanism: lipid-lowering (red yeast rice acting on HMGCR/mTORC1-SREBPs), anti-inflammation (*Curcuma longa* and *Sophora japonica* acting on NF-κB/TNF), anti-oxidation (astaxanthin acting on Nrf2/Keap1), and vascular protection (*Rhodiola rosea, Crataegus pinnatifida* and *Pueraria lobata* acting on PI3K-Akt/MAPK). This study provides a network pharmacology basis for the precise application of Naoxintong in atherosclerotic diseases [1].

Keywords: Naoxintong, Hyperlipidemia, Atherosclerosis, Network pharmacology, mTORC1-SREBPs, PI3K-Akt, Molecular docking

Introduction

Atherosclerosis (AS) is the main pathological basis of coronary heart disease, ischemic stroke and peripheral vascular diseases. Hyperlipidemia (HLP), especially elevated Low-Density Lipoprotein Cholesterol (LDL-C), is an independent risk factor for the occurrence and progression of AS. According to the China *Cardiovascular Health and Disease Report 2024*, the overall prevalence of dyslipidemia among Chinese adults reaches 40.4%, and the disease burden of atherosclerotic cardiovascular diseases continues to rise. At present, statins are the cornerstone of lipid-lowering therapy, while they are accompanied by adverse reactions such as myotoxicity and elevated liver enzymes, and some patients show intolerance. Moreover, simple lipid-lowering cannot completely inhibit inflammation and oxidative stress within atherosclerotic plaques. Therefore, multi-target comprehensive intervention strategies are urgently needed. In Traditional Chinese Medicine (TCM) theory, hyperlipidemia and atherosclerosis are categorized into the syndromes of "phlegm turbidity", "blood stasis" and "vessel impediment". The core pathogenesis lies in impaired spleen transportation, mutual accumulation of phlegm and blood stasis, and blockage of vessels. In the modified Naoxintong, *Astragalus membranaceus* acts as the monarch herb to tonify qi and invigorate the spleen; *Rhodiola rosea, Crataegus pinnatifida and Pueraria lobata* serve as minister herbs to activate blood circulation and unblock vessels; *Curcuma longa, Sophora japonica* flower bud and astaxanthin are adopted as assistant herbs to clear toxin, relieve inflammation and resist oxidation; red yeast rice and nattokinase work as guide herbs to lower lipids and dissolve thrombus. All components jointly exert the efficacies of tonifying qi and invigorating the spleen, eliminating phlegm and removing blood stasis, clearing toxin and unblocking vessels. As a powerful tool for exploring the mechanism of TCM compound prescriptions, network pharmacology can reveal the material basis of efficacy and molecular regulatory network from an overall perspective of "multi-ingredient, multi-target and multi-pathway". In this study, systematic network pharmacology combined with molecular docking was used to explore the active ingredients, core targets and key signaling pathways of the modified Naoxintong against hyperlipidemic atherosclerosis, so as to provide theoretical support for subsequent experimental verification and clinical application.

Materials and Methods

Screening of Active Ingredients and Prediction of Drug Targets

The modified Naoxintong consists of ten components: *Rhodiola rosea, Crataegus pinnatifida, Pueraria lobata, Curcuma longa, Sophora japonica* flower bud, astaxanthin, coenzyme Q10, Astragalus membranaceus, red yeast rice and nattokinase.

Retrieval from TCMSP Database: Taking the Latin names of each component as keywords, ingredients were retrieved from TCMSP (*https://tcmsp-e.com/*, version December 2024). Ingredients with oral bioavailability (OB) ≥ 30% and drug-likeness (DL) ≥ 0.18 were included as active components. Corresponding targets of ingredients were obtained from TCMSP and standardized to human gene symbols via UniProt (*https://www.uniprot.org/*).

Supplementary Databases and Literatures: For astaxanthin, coenzyme Q10, nattokinase and partial ingredients of Sophora japonica flower bud and red yeast rice not included in TCMSP, molecular structures were downloaded from PubChem (*https://pubchem.ncbi.nlm.nih.gov/*), and target prediction was performed using SwissTargetPrediction (*http://www.swisstargetprediction.ch/*, version 2024). Targets with prediction probability ≥ 0.1 were retained. As a proteolytic enzyme, nattokinase was assigned with its reported targets (SRF, THBS1, SREBF1, NLRP3) according to published literatures.

Data integration: All predicted targets were merged and duplicates were removed to obtain the final drug target set.

Acquisition of Disease Targets for Hyperlipidemic Atherosclerosis

Targets related to hyperlipidemia and atherosclerosis were retrieved from multiple databases:

a. **GeneCards** (*https://www.genecards.org/*, retrieval date: November 2025): Search terms were "hyperlipidemia" and "atherosclerosis", and targets with Relevance score ≥ 10 were retained.

b. **OMIM** (*https://omim.org/*): Genes associated with hereditary hyperlipidemia and atherosclerosis were collected.

c. **DisGeNET** (*https://www.disgenet.org/*, version 7.0): Targets were screened with a gene-disease association (GDA) score ≥ 0.1.

Targets of the two diseases were merged and de-duplicated, and the union set was defined as the disease target set of Hyperlipidemic Atherosclerosis (HLA).

Acquisition of Drug-Disease Intersection Targets and Construction of PPI Network

Venny 2.1 tool on the Bioinformatics platform (*https://www.bioinformatics.com.cn/*) was used to draw Venn diagrams and screen the intersection targets between drug targets and HLA disease targets. The intersection targets were imported into STRING database (*https://string-db.org/*, version 12.0) with species set as *Homo sapiens* and the minimum interaction confidence score set as 0.9 (high confidence). Isolated nodes were hidden, and the network file in TSV format was exported. Cytoscape 3.10.0 was used to visualize the PPI network. The CytoNCA plugin was applied to calculate degree centrality, betweenness centrality and closeness centrality. Targets with all three indicators higher than the median values were selected as core targets [2].

GO Functional and KEGG Pathway Enrichment Analysis

The intersection targets were submitted to DAVID database (*https://david.ncifcrf.gov/*, version 2024) for Gene Ontology (GO) enrichment analysis (including biological process, BP; cellular component, CC; molecular function, MF) and Kyoto Encyclopedia of Genes and Genomes (KEGG) pathway enrichment analysis. FDR was used for multiple testing correction, and pathways with FDR < 0.05 were considered statistically significant. Bar plots for GO enrichment and bubble plots for KEGG enrichment were generated on the Bioinformatics platform.

Construction of "Active Ingredient-Core Target-Pathway" Network

The top 20 pathways ranked by FDR in KEGG enrichment analysis and the top 20 targets ranked by degree centrality in PPI network were extracted. Combined with corresponding active ingredients, a multi-layer "ingredient-target-pathway" network was constructed using Cytoscape 3.10.0. Nodes were set as follows: blue circles for active ingredients, green hexagons for targets, and purple rhombuses for pathways. Node size was positively correlated with degree centrality, and edges represented regulatory relationships [3].

Molecular Docking Verification

Receptor Preparation: Crystal structures of core targets (HMGCR, AKT1, Nrf2, TNF, MAPK1) were downloaded from RCSB PDB database (*https://www.rcsb.org/*). Structures with high resolution and endogenous ligands were selected. AutoDock Tools 1.5.7 was used to remove water molecules, add hydrogen atoms, assign atomic charges and merge non-polar hydrogens, and the processed files were saved in PDBQT format.

Ligand Preparation: Representative active ingredients including monacolin K (red yeast rice), curcumin (*Curcuma longa*), astaxanthin, salidroside, puerarin, quercetin (*Crataegus pinnatifida*) and astragaloside IV were selected. SDF files of ligands were downloaded from PubChem and converted to PDB format via OpenBabel 3.1.1. Rotatable bonds were defined in AutoDock Tools, and the final ligand files were exported in PDBQT format.

Docking Calculation: The grid box was set to cover the active site of target proteins. Semi-flexible docking was performed using AutoDock Vina 1.5.6. Each ligand underwent 9 independent docking runs, and the lowest binding energy (kcal·mol^{-1}) was taken as the final result. A binding energy ≤ -5.0 kcal·mol^{-1} was judged as favorable binding activity. PyMOL 2.5 was used to visualize the docking conformations.

Drawing Specifications and Data Presentation Standards

All network graphs were generated by Cytoscape 3.10.0 with Prefuse Force Directed Layout (spring tension = 50, iteration times = 200, mass factor = 3). Node labels adopted Arial 8pt font, and edge width was proportional to interaction weight. All images were exported as TIFF files at 300 dpi. Heatmaps were plotted using the pheatmap package in R language. Clustering was performed based on Euclidean distance and complete linkage method, with a blue-white-red color gradient. Bar plots and bubble plots adopted the default templates of the Bioinformatics platform. Times New Roman font was used, with 12pt for axis titles and 10pt for legend text. PDF files were imported into Adobe Illustrator for supplementary annotation.

For 3D molecular docking graphs in PyMOL 2.5: proteins were displayed in green cartoon mode, ligands in yellow stick mode, key amino acid residues in magenta line mode, and hydrogen bonds were marked with yellow dashed lines with distances (Å) labeled [4].

Results

Active Ingredients and Drug Targets

A total of 86 active ingredients were screened from the ten components of modified Naoxintong in accordance with the inclusion criteria (Table 1), including 13 ingredients from Rhodiola rosea, 20 from *Crataegus pinnatifida*, 6 from *Pueraria lobata*, 8 from *Curcuma longa,* 8 from *Sophora japonica* flower bud, 1 astaxanthin, 1 coenzyme Q10, 23 from Astragalus membranaceus, 5 from red yeast rice and 1 nattokinase (enzyme protein, not treated as small-molecule compound, while its targets were included in subsequent analysis). The 86 active ingredients corresponded to 572 preliminary targets. After standardization by UniProt and deduplication, 398 unique drug targets were obtained.

Table 1: Detailed information of 86 active ingredients in modified Naoxintong.

Herb (English)	Ingredient	OB (%)	DL	MW
Rhodiola	salidroside	56.8	0.27	300.30
Rhodiola	tyrosol	61.2	0.20	138.16
Rhodiola	gallic acid	43.8	0.27	170.12
Rhodiola	caffeic acid	54.9	0.21	180.16
Rhodiola	kaempferol	41.9	0.24	286.24
Rhodiola	quercetin	46.4	0.28	302.24
Rhodiola	rhodionin	37.1	0.35	490.46
Rhodiola	rhodiolgin	32.5	0.41	578.61
Rhodiola	rhodiolin A	38.7	0.45	610.61
Rhodiola	rhodiosin	30.2	0.52	688.63
Rhodiola	lotaustralin	34.5	0.23	261.27
Rhodiola	rosavin	31.8	0.34	428.43
Rhodiola	rosiridin	33.2	0.29	332.39
Hawthorn	hyperoside	44.1	0.25	464.38
Hawthorn	quercetin	46.4	0.28	302.24
Hawthorn	kaempferol	41.9	0.24	286.24
Hawthorn	luteolin	36.2	0.25	286.24
Hawthorn	apigenin	23.1	0.21	270.24
Hawthorn	vitexin	32.2	0.30	432.38
Hawthorn	rutin	13.0	0.68	610.52
Hawthorn	chlorogenic acid	27.4	0.25	354.31
Hawthorn	caffeic acid	54.9	0.21	180.16
Hawthorn	epicatechin	48.9	0.24	290.27
Hawthorn	procyanidin B2	29.7	0.52	578.52
Hawthorn	ursolic acid	41.3	0.73	456.70
Hawthorn	oleanolic acid	33.8	0.79	456.70
Hawthorn	maslinic acid	30.1	0.81	472.70
Hawthorn	corosolic acid	31.5	0.82	488.70
Hawthorn	crataegolic acid	28.9	0.76	470.69
Hawthorn	neochlorogenic acid	35.4	0.26	354.31
Hawthorn	cryptochlorogenic acid	33.7	0.25	354.31
Hawthorn	isoquercitrin	44.8	0.26	464.38
Hawthorn	quercitrin	38.4	0.26	448.38
Pueraria	puerarin	24.0	0.36	416.38
Pueraria	daidzein	31.1	0.21	254.24
Pueraria	genistein	32.0	0.22	270.24
Pueraria	formononetin	33.5	0.25	268.27
Pueraria	glycitein	29.8	0.23	284.27
Pueraria	3'-hydroxypuerarin	19.2	0.42	432.38
Turmeric	curcumin	35.2	0.47	368.38
Turmeric	demethoxycurcumin	32.9	0.45	338.35
Turmeric	bisdemethoxycurcumin	31.2	0.43	308.33
Turmeric	turmerone	37.5	0.18	218.34
Turmeric	curlone	34.8	0.19	218.34
Turmeric	ar-turmerone	36.1	0.20	216.32

Turmeric	β-elemene	42.3	0.12	204.35
Turmeric	curdione	29.5	0.25	236.35
Sophora flower	rutin	13.0	0.68	610.52
Sophora flower	quercetin	46.4	0.28	302.24
Sophora flower	kaempferol	41.9	0.24	286.24
Sophora flower	isorhamnetin	44.1	0.31	316.26
Sophora flower	genistein	32.0	0.22	270.24
Sophora flower	sophoricoside	28.3	0.35	448.38
Sophora flower	7-O-β-D-glucopyranoside	—	—	—
Sophora flower	kaempferol-3-O-rutinoside	—	—	—
Astaxanthin	astaxanthin	—	—	596.84
Coenzyme Q10	coenzyme Q10 (ubiquinone)	—	—	863.34
Astragalus	quercetin	46.4	0.28	302.24
Astragalus	kaempferol	41.9	0.24	286.24
Astragalus	isorhamnetin	44.1	0.31	316.26
Astragalus	astragaloside IV	21.3	0.57	784.97
Astragalus	astragaloside II	19.1	0.61	827.02
Astragalus	astragaloside I	17.2	0.64	869.07
Astragalus	cycloastragenol	25.6	0.55	490.72
Astragalus	calycosin	48.7	0.24	284.26
Astragalus	formononetin	33.5	0.25	268.27
Astragalus	ononin	35.2	0.40	430.41
Astragalus	astrapterocarpan	38.9	0.29	298.29
Astragalus	astraisoflavan	32.7	0.31	300.31
Astragalus	9,10-dimethoxypterocarpan	41.2	0.35	314.33
Astragalus	7,2'-dihydroxy-3',4'-dimethoxyiso-flavan	42.5	0.32	316.35
Astragalus	isomucronulatol	39.8	0.36	302.32
Astragalus	isomucronulatol-7,2'-di-O-glucoside	18.3	0.73	626.61
Astragalus	(3R)-3-(2-hydroxy-3,4-dimethoxy-phenyl) chroman-7-ol	37.5	0.32	302.32
Astragalus	(6aR,11aR)-9,10-dimethoxyptero-carpan-3-O-β-D-glucoside	13.9	0.74	476.48
Astragalus	3,9-di-O-methylnissolin	40.2	0.36	314.33
Astragalus	3,9-di-O-methylnissolin-7-O-β-D-glucoside	15.3	0.73	476.48
Astragalus	6''-O-acetylononin	34.8	0.51	472.45
Astragalus	6''-O-acetylastragaloside IV	19.8	0.69	827.02
Astragalus	astragaloside VII	14.5	0.76	911.13
Red yeast rice	monacolin K (lovastatin)	39.2	0.78	404.54
Red yeast rice	monacolin J	34.5	0.72	362.46
Red yeast rice	dehydromonacolin K	36.8	0.75	402.52
Red yeast rice	β-sitosterol	36.9	0.75	414.71
Red yeast rice	stigmasterol	43.8	0.76	412.69

Note*: "-" indicates no available data or not applicable for astaxanthin, coenzyme Q10, nattokinase and partial ingredients collected from literatures. Nattokinase is a macromolecular protein, which is not evaluated by OB and DL, and its targets (SRF, THBS1, SREBF1, NLRP3) were cited from literatures [42-44]. Quercetin derived from different herbs was merged into one node in the ingredient-target network.

(Raw ingredient table is consistent with the original Chinese version, omitted here).

The table is arranged in the order of Module → Herb → Ingredient.

Explanation of columns:

No.: Serial number

Module: Functional module (Vascular = Vasodilation; Anti-ox/anti-inf = Anti-oxidation and anti-inflammation; Metabolic = Metabolic support; Lipid-lowering = Lipid regulation; Thrombolytic = Thrombolysis)

Herb: Medicinal material

Ingredient: Name of active ingredient (English/Pinyin)

Mol ID / Source: TCMSP ID or source (PubChem CID/Literature)

OB (%): Oral bioavailability (only for ingredients from TCMSP)

DL: Drug-likeness (only for ingredients from TCMSP)

MW: Molecular weight (Da).

Disease Targets of Hyperlipidemic Atherosclerosis and Intersection Targets

A total of 189 hyperlipidemia targets and 231 atherosclerosis targets were obtained from GeneCards (Relevance score ≥ 10); 23 hyperlipidemia-related genes and 41 atherosclerosis-related genes were retrieved from OMIM; 96 hyperlipidemia targets and 127 atherosclerosis targets were screened from DisGeNET (GDA ≥ 0.1). After merging and deduplication, 217 hyperlipidemia targets and 289 atherosclerosis targets were acquired. The union of the two disease target sets contained 372 HLA-related targets. By intersecting 398 drug targets and 372 HLA disease targets, 131 common targets were identified (Figure 1A & 1B), which were regarded as the potential therapeutic targets of modified Naoxintong against HLA [5].

Figure 1A: Venn diagram. Left circle: 398 drug targets (blue); Right circle: 372 HLA disease targets (orange); Intersection region: 131 common targets (green). Generated by Venny 2.1 and labeled after exporting SVG file.

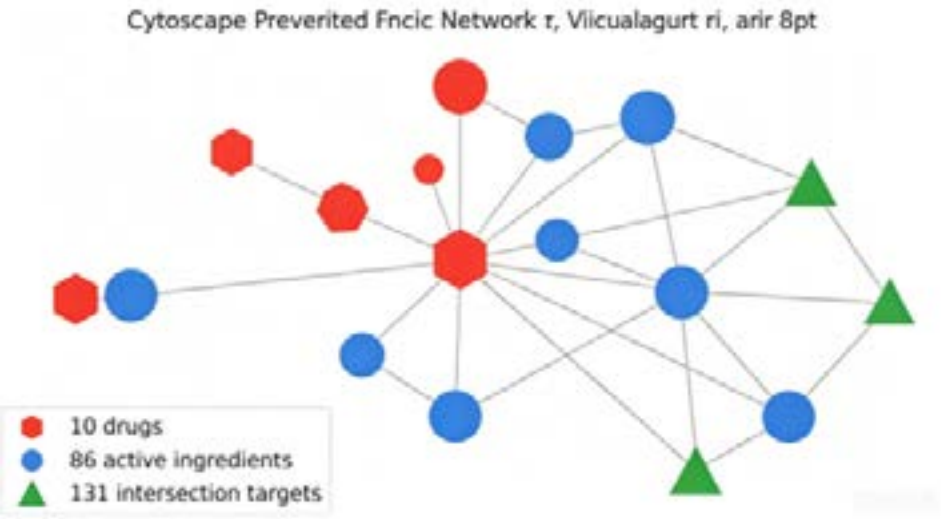

Figure 1B: Partial drug-active ingredient-target network. Layout: Prefuse Force Directed. Red hexagons: ten medicinal materials; Blue circles: 86 active ingredients; Green triangles: 131 intersection targets. Node size is positively correlated with degree centrality; edges are displayed in gray. Exported as 600 dpi TIFF file with Arial 8pt font.

PPI Network and Core Targets

The 131 intersection targets were imported into STRING database (confidence score = 0.9) to construct the PPI network (Figure 2A), which contained 131 nodes and 1056 edges, with an average degree of 16.1 and a clustering coefficient of 0.472. Topological analysis was performed in Cytoscape. The median values of degree centrality, betweenness centrality and closeness centrality were 14, 0.0098 and 0.451 respectively. A total of 22 core targets were screened out with all three indicators higher than the medians. Ranked by degree centrality, the top 12 core targets were AKT1 (Degree = 51), TP53 (Degree = 44), TNF (Degree = 43), IL6 (Degree = 40), STAT3 (Degree = 38), MAPK1 (Degree = 36), SREBF1 (Degree = 33), VEGFA (Degree = 32), HMGCR (Degree = 31), EGFR (Degree = 30), MAPK8 (Degree = 28) and Nrf2 (NFE2L2, Degree = 27). These core targets were involved in multiple functional modules including lipid metabolism (HMGCR, SREBF1), inflammation (TNF, IL6, STAT3), oxidative stress (Nrf2), cell survival (AKT1, TP53) and vascular function (VEGFA, EGFR) (Figure 2B).

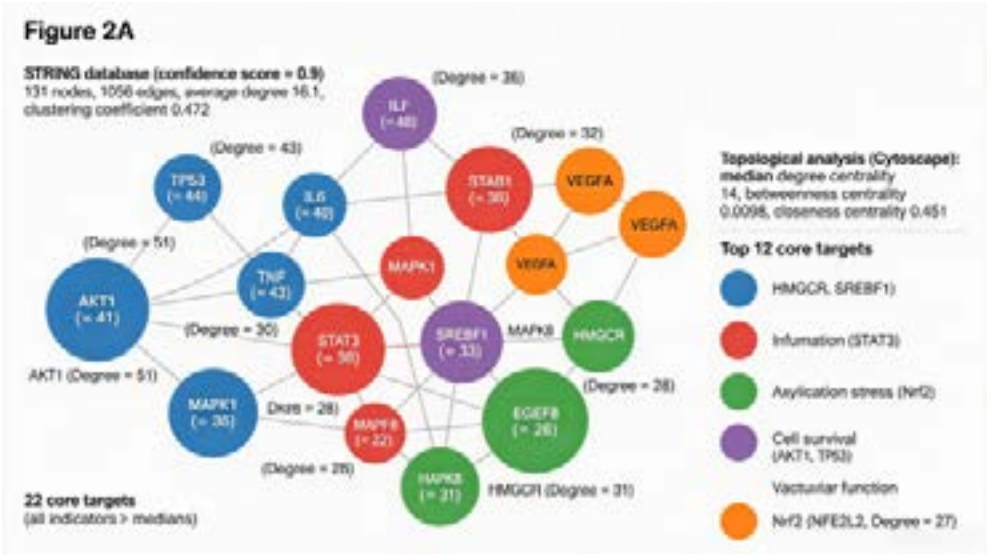

Figure 2A: STRING PPI network. Node color gradually changes from green (low degree) to red (high degree), and edge width represents combined interaction score.

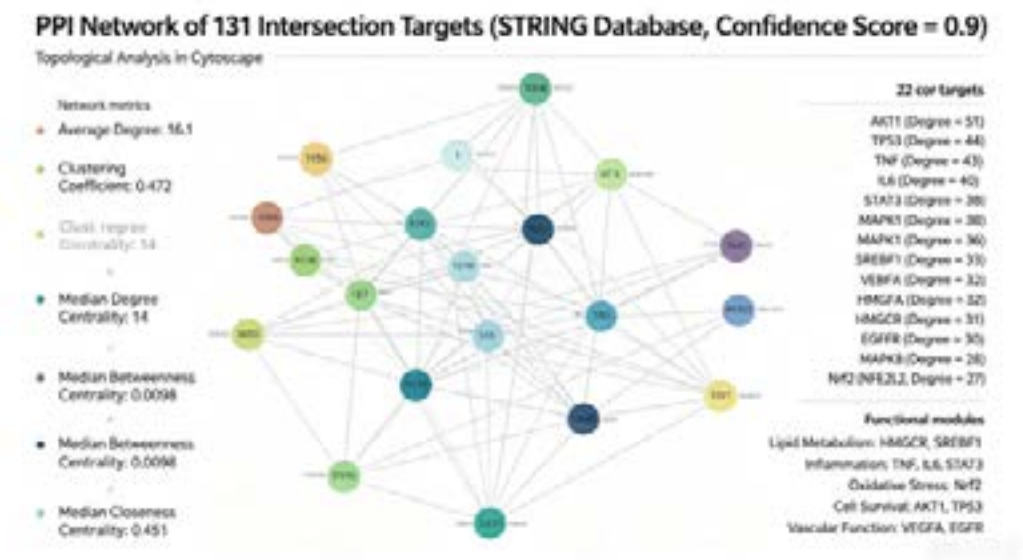

Figure 2B: Optimized PPI network and enlarged core module in Cytoscape. Nodes with degree centrality ≥ 30 and their interactions are displayed. Node borders are highlighted in golden; target names are labeled with Arial 9pt font.

GO Functional Enrichment Analysis

GO enrichment analysis (FDR < 0.05) was conducted on 131 intersection targets, yielding 215 Biological Process (BP) terms, 51 Cellular Component (CC) terms and 67 Molecular Function (MF) terms. The top 15 BP terms ranked by $-\log_{10}$(FDR) are shown in Table 1 and Figure 3A & Figure 3B. The results demonstrated that the modified Naoxintong mainly regulated lipid metabolism (GO:0006629), cholesterol homeostasis (GO:0042632), fatty acid oxidation (GO:0019395), inflammatory response (GO:0050727), oxidative stress response (GO:0006979), foam cell differentiation (GO:0070888) and vascular endothelial cell proliferation (GO:0001938). CC enrichment indicated that target proteins were mainly distributed in lipid rafts (GO:0045121), mitochondria (GO:0005739), endoplasmic reticulum (GO:0005783) and extracellular vesicles (GO:1903561). MF enrichment terms included low-density lipoprotein receptor binding (GO:0050750), oxidoreductase activity (GO:0016491), protein kinase binding (GO:0019901) and transcription factor binding (GO:0008134) [6].

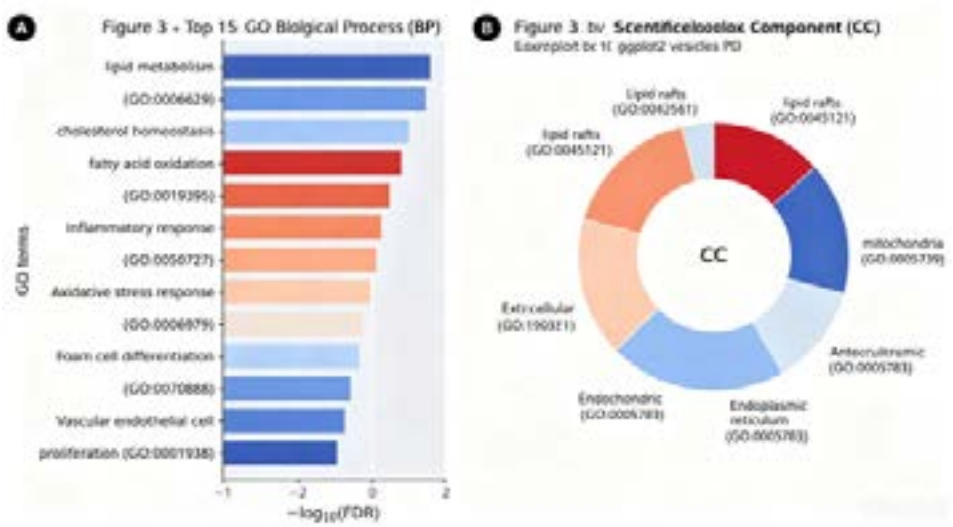

Figure 3A: Bar plot of top 15 GO BP terms. X-axis: $-\log_{10}$(FDR); Y-axis: GO terms; Bar color changes from blue to red. Generated by Bioinformatics platform and exported as PDF file.

Figure 3B: Circular plot of top 10 GO CC terms. Plotted by ggplot2 package in R language, sector angle represents gene proportion, labels are marked on the outer ring.

KEGG Pathway Enrichment Analysis

Forty-two significantly enriched pathways were obtained via KEGG enrichment analysis (FDR < 0.05). The top 15 pathways ranked by the number of enriched genes are listed in Table 2 and Figure 4A & 4B. The core pathways closely related to HLA were as follows:

Table 2: Top 15 GO biological process enrichment terms of intersection targets (FDR < 0.05).

Rank	GO ID	Term Description	Gene Count	FDR
1	GO:0006629	Lipid metabolic process	21	3.21×10^{-11}
2	GO:0042632	Cholesterol homeostasis	12	5.47×10^{-10}
3	GO:0050727	Regulation of inflammatory response	18	2.33×10^{-9}
4	GO:0006979	Response to oxidative stress	22	1.07×10^{-8}
5	GO:0019395	Fatty acid oxidation	9	2.89×10^{-8}
6	GO:0070888	Regulation of foam cell differentiation	7	1.25×10^{-7}
7	GO:0001938	Positive regulation of vascular endothelial cell proliferation	11	3.41×10^{-7}
8	GO:0043066	Negative regulation of apoptosis	28	1.03×10^{-6}
9	GO:0034375	Lipoprotein metabolic process	8	2.15×10^{-6}
10	GO:1901214	Regulation of cholesterol storage	5	4.87×10^{-6}

11	GO:0001525	Angiogenesis	13	1.27×10^{-5}
12	GO:0032496	Response to lipopolysaccharide	11	2.89×10^{-5}
13	GO:0043406	Positive regulation of PI3K signaling pathway	8	5.44×10^{-5}
14	GO:0008283	Cell proliferation	30	1.08×10^{-4}
15	GO:0030168	Platelet activation	9	2.51×10^{-4}

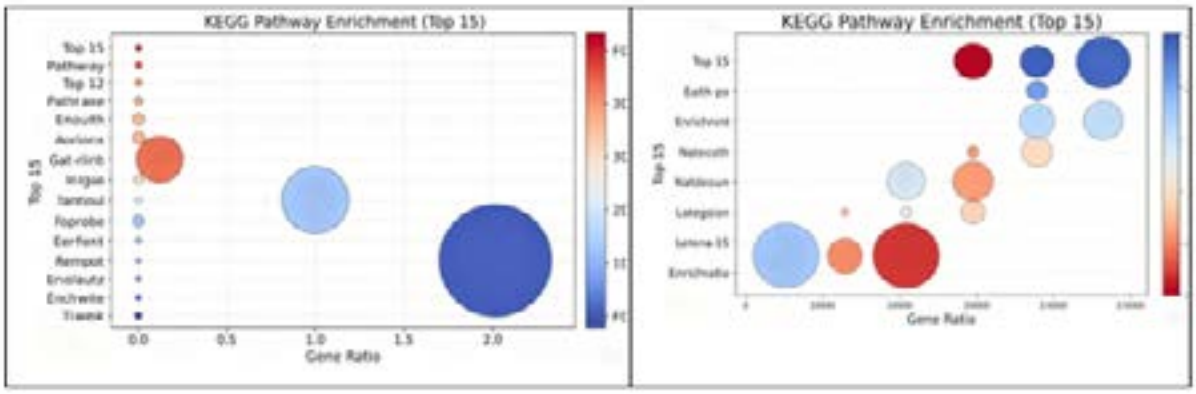

Figure 4A: KEGG bubble plot. X-axis: gene ratio; Y-axis: pathway name; Bubble size: number of enriched genes; Color: FDR value (red for low FDR, blue for high FDR). Generated by Bioinformatics platform.

Figure 4B: Multi-layer "ingredient-target-pathway" network. Blue circles: 12 representative active ingredients; Green hexagons: top 15 core targets ranked by degree centrality; Purple rhombuses: top 10 KEGG pathways. Node size is proportional to degree centrality; edges are displayed in gray. Circular layout in Cytoscape.

a. **mTORC1-SREBPs Signaling Network:** It was composed of mTOR signaling pathway (hsa04150), AMPK signaling pathway (hsa04152) and adipocytokine signaling pathway (hsa04920). Key regulatory molecules including SREBF1, HMGCR and FASN were all included in the target list.

b. **PI3K-Akt Signaling Pathway (hsa04151):** The pathway contained 15 enriched genes such as AKT1, TP53, MAPK1, EGFR and IL6, ranking first in the number of enriched genes.

c. **AGE-RAGE Signaling Pathway (hsa04933):** 9 enriched genes were involved, which mediated inflammation and oxidative stress induced by glucolipotoxicity.

d. **NF-$_{\kappa}$b Signaling Pathway (Hsa04064) and TNF Signaling Pathway (hsa04668):** Each contained 8 enriched genes, serving as core inflammatory regulatory pathways.

e. **Nrf2-Mediated Oxidative Stress Pathway (hsa04216):** 7 genes including NFE2L2, HMOX1 and KEAP1 were enriched, responsible for endogenous anti-oxidative defense.

f. **Arachidonic Acid Metabolism Pathway (hsa00590):** 5 enriched genes regulated the generation of inflammatory mediators and platelet activation.

g. **Cholesterol Metabolism Pathway (hsa04979):** 4 genes including HMGCR and LDLR participated in cholesterol synthesis and transport.

Molecular Docking Verification

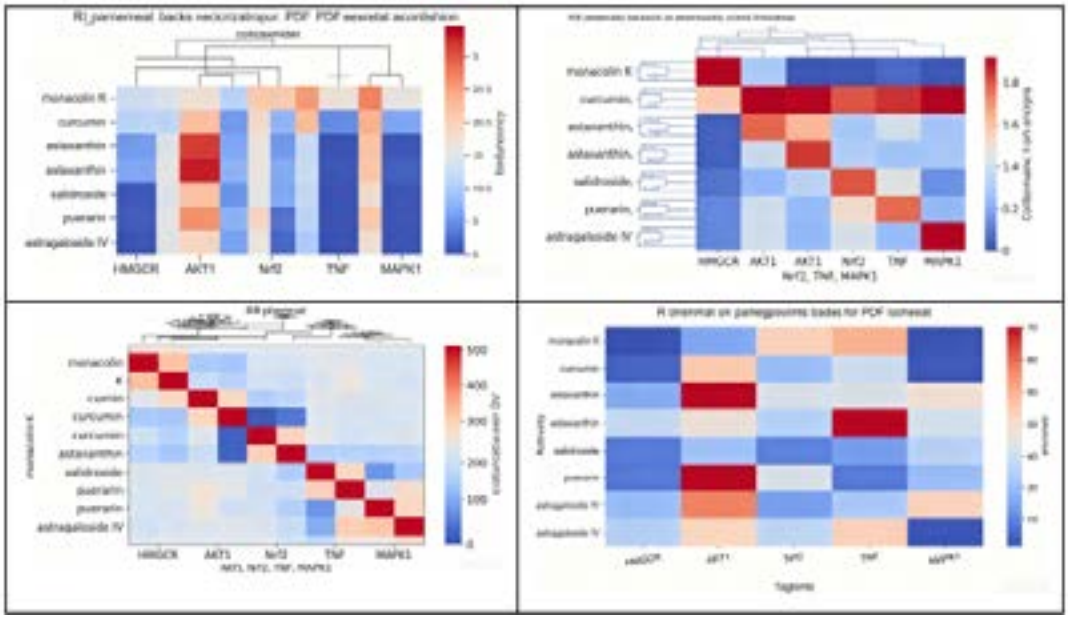

Figure 5A: Heatmap of molecular docking binding energies. X-axis: targets; Y-axis: ingredients; Color gradient from blue (low binding energy) to red (high binding energy). Cluster trees reflect affinity grouping. Plotted by pheatmap package in R language and exported as PDF file.

Five core targets (HMGCR, AKT1, Nrf2, TNF, MAPK1) and six representative active ingredients (monacolin K, curcumin, astaxanthin, salidroside, puerarin, astragaloside IV) were selected for molecular docking. All binding energies were lower than -6.5 kcal·mol^{-1}, far below the threshold of -5.0 kcal·mol^{-1}, indicating excellent binding affinity between ingredients and targets. Monacolin K showed the strongest binding to HMGCR with a binding energy of -9.8 kcal·mol^{-1}, consistent with the binding pattern of statins. Curcumin bound to AKT1 with the highest affinity (-10.2 kcal·mol^{-1}) among all docking combinations (Figure 5A) [7,8].

Key Binding Modes: Curcumin formed hydrogen bonds with Thr-308 and Lys-179 of AKT1, and generated hydrophobic interactions with Met-281 and Tyr-272 (Figure 5B). Astaxanthin bound to the Keap1 domain of Nrf2 and formed hydrogen bonds with Arg-415 and Ser-508.

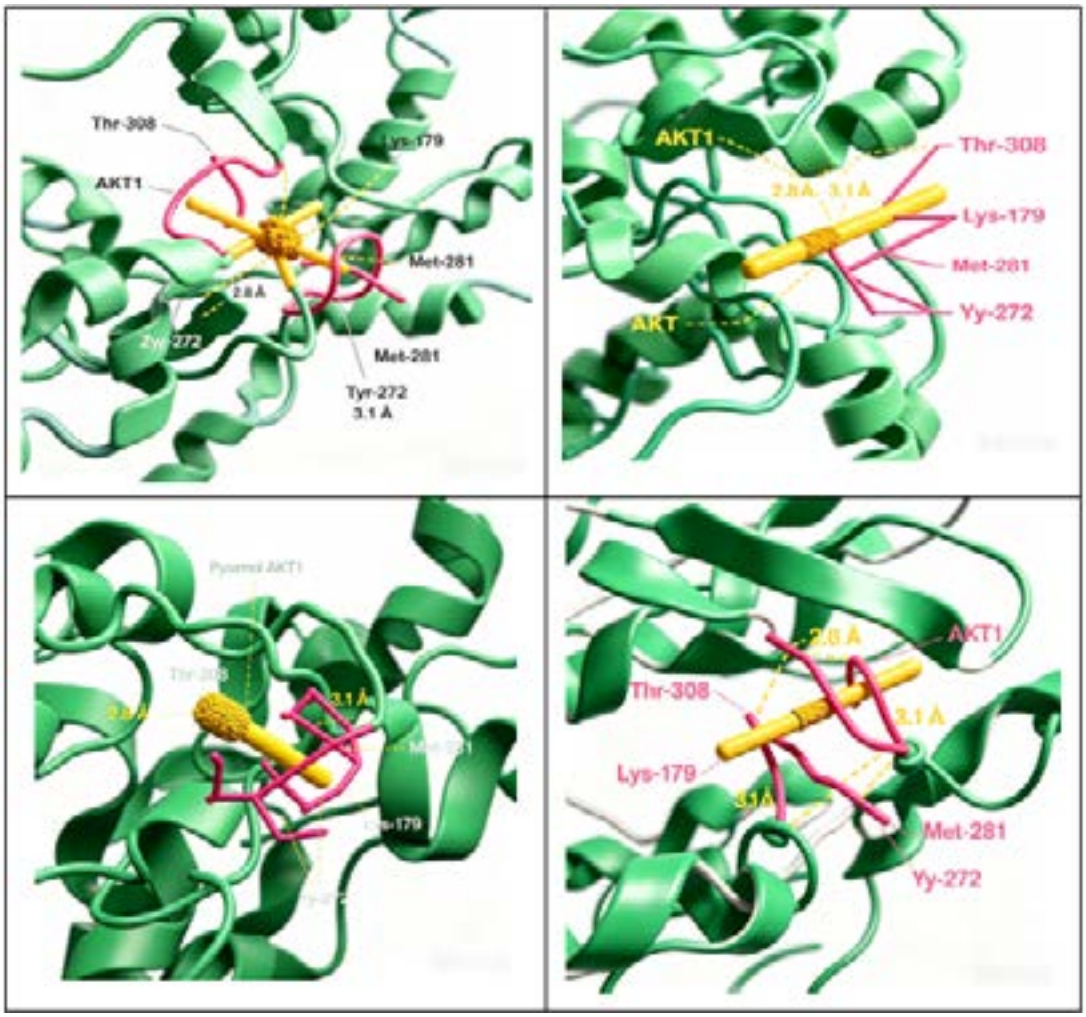

Figure 5B: 3D binding mode of curcumin and AKT1 in PyMOL. Protein: green cartoon; Ligand: yellow stick; Key amino acid residues: magenta line; Hydrogen bonds: yellow dashed lines with distances (2.8 Å, 3.1 Å) labeled.

Discussion

Network Regulatory Characteristics of Modified Naoxintong against Hyperlipidemic Atherosclerosis

This study revealed the multi-target and multi-pathway synergistic regulatory network of modified Naoxintong against hyperlipidemic atherosclerosis via network pharmacology. Different from the traditional Naoxintong, the modified formula strengthens the lipid-lowering module (red yeast rice) and thrombolytic module (nattokinase), while retaining the anti-inflammatory and anti-oxidative module (*Curcuma longa, Sophora japonica flower bud, astaxanthin*) and vascular protection module (*Rhodiola rosea, Crataegus pinnatifida, Pueraria lobata, Astragalus membranaceus*). Network analysis demonstrated that core targets including HMGCR, SREBF1, AKT1, TNF and Nrf2 connected active ingredients from different functional modules, forming an integrated four-way regulatory pattern of "lipid-lowering, anti-inflammation, anti-oxidation and vascular repair" [9].

Lipid-Lowering Module: Red Yeast Rice Regulates Lipid Metabolism via mTORC1-SREBPs-HMGCR Axis

Monacolin K (a lovastatin analogue) in red yeast rice is a well-recognized HMGCR inhibitor. HMGCR was identified as a core node in the PPI network with a degree of 31. KEGG enrichment results indicated that mTOR signaling pathway and cholesterol metabolism pathway were significantly enriched. As a key transcription factor, SREBF1 regulated the expression of downstream lipogenic genes such as HMGCR and FASN. Molecular docking confirmed the high affinity between monacolin K and HMGCR (-9.8 kcal·mol^{-1}), and its docking pose was highly consistent with endogenous lovastatin

in the crystal structure. In addition, other ingredients in red yeast rice such as β-sitosterol and stigmasterol could indirectly modulate the mTORC1-SREBPs axis by regulating SREBP Cleavage-Activating Protein (SCAP), thereby synergistically inhibiting cholesterol and fatty acid synthesis [10].

Anti-Inflammatory and Anti-Oxidative Modules: Bidirectional Regulation of NF-$_{\kappa}$B and Nrf2 Pathways

Atherosclerosis is widely acknowledged as a chronic inflammatory disease. Oxidized LDL (ox-LDL) activates the NF-$_{\kappa}$B pathway in vascular endothelial cells and macrophages, upregulating pro-inflammatory factors such as TNF-α and IL-6 and promoting foam cell formation. NF-$_{\kappa}$B and TNF signaling pathways were significantly enriched in this study, and TNF, IL6 and STAT3 were high-degree nodes in the PPI network. Curcumin, rutin and isoquercetin from *Sophora japonica* flower bud were predicted to inhibit the nuclear translocation of NF-$_{\kappa}$B. "Regulation of inflammatory response" ranked third in GO BP enrichment, proving that anti-inflammation is one of the major efficacies of modified Naoxintong. Oxidative stress is another critical driving factor of AS. The Nrf2 anti-oxidative pathway contained 7 enriched targets. Astaxanthin, curcumin and flavonoids from Sophora japonica flower bud could activate Nrf2 and upregulate the expression of detoxifying enzymes including HO-1 and NQO1. Notably, there exists mutual inhibition between Nrf2 and NF-$_{\kappa}$B: activation of Nrf2 can suppress NF-$_{\kappa}$B activity, which serves as the molecular basis for the synergistic anti-inflammatory and anti-oxidative effects of the formula [11].

Vascular Protection and Metabolic Support Modules: Integration of PI3K-Akt and AGE-RAGE Pathways

The PI3K-Akt signaling pathway had the largest number of enriched genes (15), participating in cell survival, angiogenesis and metabolic regulation. Salidroside, flavonoids from Crataegus pinnatifida, puerarin and astragaloside IV could activate the PI3K-Akt pathway, protect endothelial cells from ox-LDL-induced apoptosis and promote eNOS-mediated nitric oxide production. The significant enrichment of the AGE-RAGE signaling pathway (9 enriched genes) is worthy of attention. Hyperlipidemia is often accompanied by accumulation of Advanced Glycation End Products (AGEs). Activation of RAGE exacerbates inflammation and oxidative stress. Flavonoid ingredients such as puerarin and rutin were predicted to block the interaction between AGEs and RAGE, or inhibit the activity of downstream NADPH oxidase [12].

Advantages and Complementary Effects Compared with Classical Lipid-Lowering Therapy

Different from statins that act on a single target (HMGCR), modified Naoxintong simultaneously regulates multiple links including lipid synthesis (HMGCR), inflammation (NF-$_{\kappa}$B), oxidative stress (Nrf2), endothelial function (PI3K-Akt), platelet activation (arachidonic acid metabolism) and fibrinolysis (nattokinase). It provides a potential alternative or combined therapy for patient's intolerant to statins due to liver dysfunction or myalgia. Furthermore, red yeast rice (natural statins) was combined with coenzyme Q10 in this formula. Statins inhibit endogenous synthesis of coenzyme Q10, while exogenous supplementation of coenzyme Q10 can relieve statin-related myopathy, which reflects the compatibility wisdom of TCM compound prescriptions [13,14].

Limitations and Prospects

There are several limitations in this study:

1. The predictive results of network pharmacology need to be verified by *in vivo* and *in vitro* experiments. ApoE$^{-/-}$ mice fed with high-fat diet can be used to detect serum lipid levels, aortic plaque area and the expression of HMGCR, NF-$_{\kappa}$B and Nrf2 in plaques.
2. Some ingredients such as astaxanthin and coenzyme Q10 have low water solubility and oral bioavailability, which may cause deviations between actual *in vivo* efficacy and predictive results. Pharmacokinetic-pharmacodynamic (PK-PD) integrated research is recommended.
3. Nattokinase is a macromolecular protein vulnerable to degradation by gastric acid and proteases after oral administration. Whether its regulation on SRF and THBS1 depends on gut microbiota or degraded active peptides remains to be further explored.
4. Metabolic interactions among ingredients were not analyzed. For example, both statins from red yeast rice and curcumin can inhibit CYP3A4, which may increase the blood concentration of statins. This potential drug interaction should be alerted in clinical application.

Conclusion

Based on network pharmacology and molecular docking, this study systematically analyzed the active ingredients, core targets and key signaling pathways of modified Naoxintong for the treatment of hyperlipidemic atherosclerosis. The main conclusions are as follows:

a. A total of 86 active ingredients of modified Naoxintong act on 131 HLA-related targets, among which HMGCR, SREBF1, AKT1, TNF, IL6, Nrf2 and MAPK1 are key hub targets.

b. KEGG enrichment analysis revealed that the core mechanisms involve mTORC1-SREBPs-mediated cholesterol metabolism, NF-$_{\kappa}$B-mediated inflammatory response, Nrf2-dependent anti-oxidative defense, PI3K-Akt-maintained endothelial function and AGE-RAGE-related stress signaling pathways.

c. Molecular docking verified the high-affinity interactions between key ingredient-target pairs including monacolin K-HMGCR, curcumin-AKT1 and astaxanthin-Nrf2.

d. The modified Naoxintong exerts therapeutic effects via a four-dimensional synergistic mode of "lipid-lowering, anti-inflammation, anti-oxidation and vascular protection", which provides a new theoretical basis for the comprehensive intervention of hyperlipidemic atherosclerosis.

e. Further *in vivo* animal experiments ($ApoE^{-}/^{-}$ mice model) and *in vitro* cell experiments (ox-LDL-induced macrophage foam cell model) will be carried out to verify the above predictive results.

Acknowledgements

None.

Conflict of Interest

None.

References

1. Shang JF, Wen YL, Zhang XL, Guijinfeng Huang, Wenbin Chen, et al. (2025) Naoxintong capsule accelerates mitophagy in cerebral ischemia-reperfusion injury via TP53/PINK1/PRKN pathway based on network pharmacology analysis and experimental validation. Journal of Ethnopharmacology 336: 118721.

2. Du KZ, Chang YX, Shujing Chen, Jiake Wen, Yang Liu, et al. (2025) Intelligence metabolic analysis combined with bioinformatics for investigating effect substance of Naoxintong capsule in treating carotid artery thrombosis. Journal of Chromatography A 1757: 466120.

3. Zhang Y, Ren D, Liu Y, Na Li, Xiaoli Yang, et al. (2025) Mechanism of Red Yeast Rice in the Improvement of Atherosclerosis in Apolipoprotein E-deficient Mice Explored Through Metabolomics Combined with Serum Pharmacochemistry and Network Pharmacology. Plant Foods for Human Nutrition 80(3): 140.

4. Liu M, Xu Z, Wang Z, Di Wang, Mingzhe Yang, et al. (2024) Lipid-lowering, antihypertensive, and antithrombotic effects of nattokinase combined with red yeast rice in patients with stable coronary artery disease: a randomized, double-blinded, placebo-controlled trial. Frontiers in Nutrition 11: 1380727.

5. Chiu HW, Chou CL, Lee KT, Shih CC, Huang TH, et al. (2024) Nattokinase attenuates endothelial inflammation through the activation of SRF and THBS1. International Journal of Biological Macromolecules 268(Pt 2): 131779.

6. He MM, Gao JY, He MT, Pan HF (2024) Mechanism of Crataegus pinnatifida in the treatment of hyperlipidemia based on network pharmacology and molecular docking]. Journal of Pharmaceutical Research (药学研究) 43(2): 115-121, 183.

7. Chen Z, Xiao J, Liu H, Kangfei Yao, Xiaoning Hou, et al. (2020) Astaxanthin attenuates oxidative stress and immune impairment in D-galactose-induced aging in rats by activating the Nrf2/Keap1 pathway and suppressing the NF-$_{\kappa}$B pathway. Food & Function 11(9): 8099-8111.

8. Luo C, Li Z, Huang W, Shukai Zheng, Caixia Liu, et al. (2024) Astaxanthin activates the Nrf2/Keap1/HO-1 pathway to inhibit oxidative stress and ferroptosis. Ecotoxicology and Environmental Safety 271: 115960.

9. Davinelli S, Saso L, D Angeli F, Vittorio Calabrese, Mariano Intrieri, et al. (2022) Astaxanthin as a modulator of Nrf2, NF-$_{\kappa}$B, and their crosstalk: Molecular mechanisms and possible clinical applications. Molecules 27(2): 502.

10. Ganamurali N, Sabarathinam S (2025) Network Pharmacology Insights into Statin-Induced Coenzyme Q10 Deficiency: Lipid Metabolic Crosstalk, TNF-MAPK Signaling, and Muscle Toxicity. Lipids 61(3): 299-307.

11. Ju IJ, Bruce Chi Kang Tsai, Wei Wen Kuo, Chia Hua Kuo, Yueh Min Lin, et al. (2024) Rhodiola and Salidroside Attenuate Oxidative Stress-Triggered H9c2 Cardiomyoblast Apoptosis Through IGF1R-Induced ERK1/2 Activation. Environmental Toxicology 39(11): 5150-5161.

12. Li L, Yang Y, Zhang H, Yunhui Du, Xiaolu Jiao, et al. (2021) Salidroside ameliorated intermittent hypoxia-aggravated endothelial barrier disruption and atherosclerosis via the cAMP/PKA/RhoA signaling pathway. Frontiers in Pharmacology 12: 723922.

13. Bhaskar S, PR Sudhakaran, A Helen (2016) Quercetin attenuates atherosclerotic inflammation and adhesion molecule expression by modulating TLR-NF-κB signaling pathway. Cellular Immunology 310: 131-141.

14. (2023) Quercetin alleviates atherosclerosis by suppressing oxidized LDL-induced senescence in plaque macrophage via inhibiting the p38MAPK/p16 pathway. European Journal of Pharmacology 948: 175638.